BULLETIN
OF THE KOREAN CHEMICAL SOCIETY

VOLUME 9, NUMBER 6
DECEMBER 20, 1988

BKCS 9(6) 333-420 (1988)
ISSN 0523-2964

Electrical Conductivity of the Spinel $CoFe_2O_4$ Solid Solution

Doo Yeon Lee, Don Kim, Keu Hong Kim*, and Jae Shi Choi

Department of Chemistry, Yonsei University, Seoul 120. *Received March 28, 1988*

Spinel $CoFe_2O_4$ solid solutions containing up to 50 mol% CoO were synthesized with spectroscopically pure CoO and α-Fe_2O_3 polycrystalline powders. The spinel structures of the $CoFe_2O_4$ solid solutions were analyzed from XRD patterns and the Mössbauer spectra showed that the quenched $CoFe_2O_4$ had a partially inversed spinel structure $(Co_{0.23}\ Fe_{0.77})\ \langle Co_{0.77}\ Fe_{1.23}\rangle O_4$, while the slowly cooled $CoFe_2O_4$ was completely inversed spinel $(Co_{0.04}\ Fe_{0.96})\ \langle Co_{0.96}\ Fe_{1.04}\rangle O_4$. The $CoFe_2O_4$ specimens containing 10,20,30 and 40 mol% CoO turned to be a mixture of corundum and spinel structures. Electrical conductivities were measured as a function of temperature from 300 to 900 °C under oxygen partial pressures from 10^{-3} to 1 atm. The temperature dependencies of the electrical conductivity show different behaviors in the low- and high-temperature regions. The average activation energies are 0.23 eV and 0.80 eV in the low- and high-temperature regions, respectively. It is suggested that $Co^{2+} \rightarrow Co^{3+} + e^-$ and $Fe^{2+} \rightleftharpoons Fe^{3+} + e^-$ are the main conduction mechanisms responsible for the electronic conduction in the low- and high-temperature regions, respectively.

Introduction

α-Fe_2O_3 has a corundum type rhombohedral structure which can be regarded as a hexagonal close packing of oxygen ions with the trivalent Fe atoms occupying 2/3 of the octahedral sites(B-sites). As the metal atoms occupy B-sites, each Fe^{3+} ion is octahedrally coordinated and surrounded by six oxygen atoms, while each oxygen is surrounded by four Fe^{3+} ions. The oxide has been reported to be either *p*-type or *n*-type semiconductor due to impurity effects [1-4]. Several investigators [5-8] have suggested that the predominating point defect in hematite is an oxygen vacancy, whereas Salomon [6] and Lord and Parker[9] reported that interstitial Fe^{3+} ions or excess metals are responsible for point defects. Bosman *et al.*[10] observed that the electrical conductivities of hematite at 400-900 °C are essentially dependent on the oxygen partial pressure. But Tannhauser [1] and Wagner *et al.* [11] reported hematite to be independent of oxygen partial pressure at 1000 °C. The activation energy of Fe_2O_3 has been reported ranging from 1.01 eV to 1.18 eV [1,2,5,8].

The *p-n* transitions in pure and doped hematites have been observed at 1350 °C [1] and at 1250 °C [10], respectively. The nonstoichiometry of CoO is due to metal deficiency. Fisher *et al.* [11], Carter *et al.* [13] and Eror *et al.*[14] reported that the electrical conductivity of CoO is proportional to $(Po_2)^{1/4}$ at oxygen pressures close to 1 atm, while Makkonen [15] observed it varies as $Po_2^{1/6}$ in the temperature range 1000-1300 °C and an oxygen pressure range of $1\text{-}10^{-3}$ atm. The studies by Fisher *et al.*[12] and Eror *et al.*[14] showed that the activation energy associated with the conductivity was larger than that for hole conduction alone. It was concluded that this difference reflected an increasing mobility with temperature and that the increased mobility took place due to the hopping process. Fisher *et al.*[12] interpreted their result in terms of a small polaron hopping model. Gvishi *et al.*[16] reported that in pure and Ti-doped CoO, the Hall mobility changed from *p*- to *n*-type in the temperature range 988-1140 °C based on the Hall effect measurements. The Hall mobility of an electron is estimated to be six times larger than that of a hole.

It has been reported that $CoFe_2O_4$ has a partially inverse or completely inverse spinel structure, with the degree of inversion depending on heat treatment[17]. In case of r(the degree of inversion) = 1 the spinel structure is $(Fe^{3+})<Co^{2+}\ Fe^{3+}>O_4$, where ( ) is a tetrahedral site and < > is an octahedral site. Size of ions, the covalent bonding effect, and the crystal field stabilization energy have influence on the degree of inversion. Since Fe^{3+}, being a d^5 ion, has no crystal field stabilization energy in an octahedral site, the larger divalent ions preferentially enter the octahedral sites so the Fe^{3+} is distributed over both tetrahedral and octahedral sites. And since Co^{2+} is d^7, it has a large octahedral stabilization energy, 30.9 KJ/mol. Therefore, $CoFe_2O_4$ should have the inverse spinel structure[18]. But from Mössbauer spectra, Sawatzky *et al.*[17] reported that the slowly cooled and quenched compositions were $(Co_{0.04}\ Fe_{0.96})\ <Co_{0.96}\ Fe_{1.04}>\ O_4$ and $(Co_{0.21}\ Fe_{0.79})\ <Co_{0.79}\ Fe_{1.21}>O_4$, respectively. They suggest-

ed that a super-exchange interaction should be taken into consideration. An octahedral Fe^{3+} ion has only six tetrahedral nearest neighbors, and if a tetrahedral Fe^{3+} ion is replaced by a Co^{2+} ion, the likelihood of a super-exchange interaction will be reduced by an appreciable percentage. Therefore, the Mössbauer spectrum shows broader lines at higher temperature. Yakel[19] reported that the lattice parameter of this spinel was 0.8399 nm from synchrotron radiation diffraction data using the Cu $K\alpha$ line at 7 keV.

The distribution of cations in different crystallographic environments increases the surface heterogeneity which introduces a special catalytic activity. Hence, this spinel exhibits a wide spectrum of activity for reactions like gas oxidation[20], isotopic exchanges of O_2[21] and H_2[22], dehydrogenation and dehydration[23], oxidative dehydrogenation [24], and N_2O decomposition[25]. The spinel lattice imparts extra stability to the catalysts under various reaction conditions, such that these systems have sustained activities and selectivities for longer periods[26]. For these reasons, ferrites have been used extensively as catalysts for some industrially important processes like oxidative dehydrogenation of butenes to butadiene[27] ($MgFe_2O_4$, $ZnFe_2O_4$ etc), and hydrodesulphurization of petroleum crudes[28] ($CoFe_2O_4$). Gillot *et al.*[29] reported that in iron excess ferrites, the predominant conduction process is due to the hopping of the electron from Fe^{2+} to Fe^{3+} leading to a type of conductivity with realatively low activition energy, but in iron deficient ferrites, the dominant conduction mechanism is due to hole hopping. It was found by Jonker[30] that the ferrite $Co_{1-\delta}\ Fe_{2+\delta}\ O_4$ has two regions of conductivity. In one region of composition containing Co^{2+} and Co^{3+} ions, there is a high resistivity. In the other region of composition containing Fe^{2+} and Fe^{3+} ions there is a low resistivity. Krishnamurthy *et al.*[31] reported $CoFe_2O_4$ to be *p*-type with activation energy of 0.57 eV. But even now, no reasonable conduction mechanism has been established.

Therefore, we prepared $CoFe_2O_4$ solid solutions using α-Fe_2O_3 and CoO through a thermal reaction. The preparation technique is very simple, but has not been reported yet. Our aim is to elucidate the conduction mechanism and investigate application to other similar systems.

Experimental

Sample preparation[32, 33] and analysis. $Fe(NO_3)_2\ 9H_2O$ solution in water was added to 6% aquous ammonia under constant stirring. The precipitate was washed with distilled water until the washed liquor was free from nitrates and then dried at 80 °C. The product was heated to 240 °C for 12 hrs with a dry stream of air in order to remove the water. The phase of the product was identified by the X-ray diffractometer (XRD, Philips PW 1710) and turned to be a fine α-Fe_2O_3 phase. Atomic absorption spectroscopic data showed that the α-Fe_2O_3 powder contains less than 131 ppm of total impurities such as Cu, Mn, Ca, Co, K, etc.

Fine powder α-Fe_2O_3 and CoO (obtained from Johnson Matthey Co. 99.99%) were uniformly dispersed in mol ratios in chemically pure ethanol for 72 hrs and then dried at 200 °C. The mixtures were sintered at 1100 °C for 24 hrs in a covered platinum crucible and cooled slowly to room temperature in order to minimize the defects produced by cooling. The preheated specimen were than etched in dilute HNO_3 and $(NH_4)_2S_2O_8$. The amounts of CoO incorporated in-

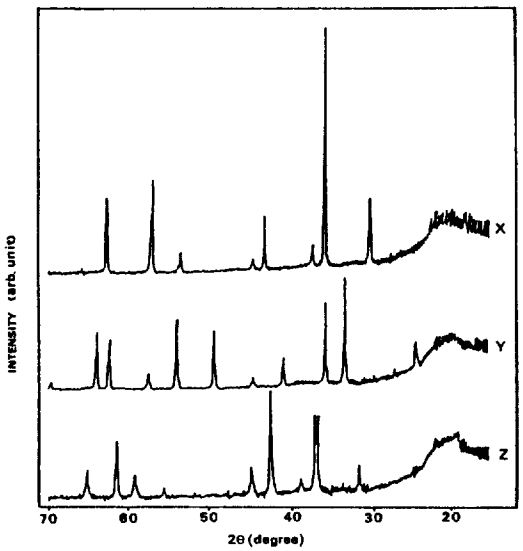

Figure 1. Comparison of the XRD peaks for slowly cooled and quenched $CoFe_2O_4$(X), α-Fe_2O_3(Y) and CoO(Z) samples.

to the α-Fe_2O_3 were determined by A.A.S. and found to be 10, 20, 30, 40, and 50 mol%, respectively. The $CoFe_2O_4$ samples were compressed into pellets under 196 MPa in vacuum and then heated to 1150 °C for 48 hrs. Some pellets were quenched with water (15 °C) and others were cooled to room temperature at a cooling rate of 50 °C/h. The pellet density measured by the mercury immersion technique was 94-96% of the theoretical density, with an average grain size of approximately 6.47 μm. The specimens had 4-6% porosity and the average pore size was approximately 0.76μm. The pellets were cut into rectangular forms, approximately $1.5 \times 0.95 \times 0.35$ cm^3 in size by diamond cutter and polished flat using α-Fe_2O_3 powder as the abrasive. Before the sample was introduced into the quartz basket, it was always etched in $(NH_4)_2\ S_2O_8$ and dilute HNO_3, washed with distilled water, dried, and then connected to the Pt probes. The Mössbauer spectra of the Fe nuclei in cobalt ferrites were recorded at 298K. The spectra were fitted by the nonlinear least square method.

Conductivity measurements. Electrical conductivities were measured using a standard four-probe configuration which has been described elsewhere[34,35]. This four-terminal method has already been emplyed to measure the resistivity of other oxide semiconductors[36-46] and polymer composites[47,48]. The current through the sample was maintained at from 10^{-10}-10^{-5} A by a rheostat, and the potential across the inner two probes was maintained between 0.5 and 1.6V. The current through the sample and the potential difference were measured by a Keithley 616 digital electrometer and by a Keithley 642 digital multimeter, respectively. The conductivity measurements were performed over a cycle in the temperature range 300-900 °C under oxygen partial pressures (Po_2) from 10^{-2} to 1 atm.

Production of Po_2. Pure oxygen or a mixture of 0.001% oxygen in nitrogen (Matheson Gas Products) was used to establish the oxygen partial pressures. The quartz sample container was first evacuated to a pressure of 1×10^{-5} torr by a diffusion pump at room temperature, and the temperature of the sample container was increased to 300 °C. A mixture of oxygen and nitrogen was introduced into the container,

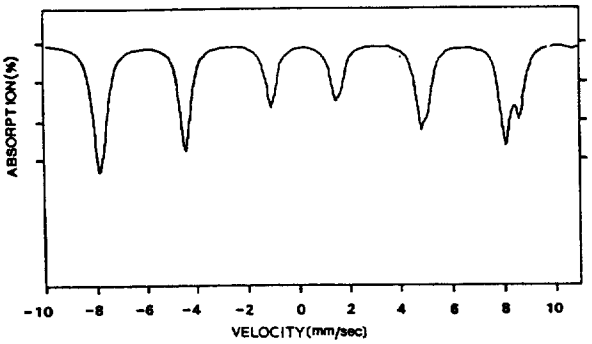

Figure 2. Mössbauer Spectrum of quenched 50 mol % $CoFe_2O_4$.

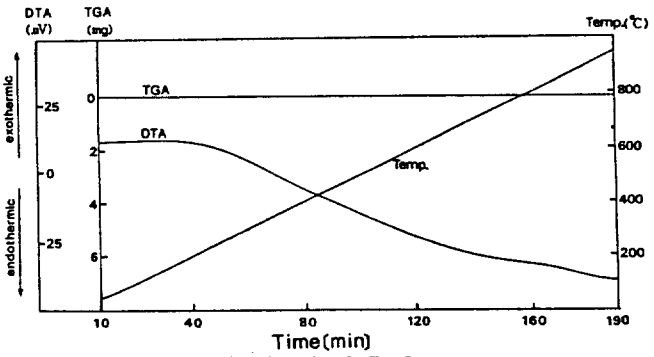

Figure 3. DTA and TGA data for $CoFe_2O_4$.

which was then evacuated again to a pressure of 1×10^{-5} torr. This procedure was repeated three or four times, and the total pressure was controlled using a mixture containing 0.001 % oxygen in nitrogen in order to establish the required Po_2. The pressures in the evacuated sample container and the mixture were read on a McLeod gauge and a manometer.

Results

XRD patterns show that the 50 mol% $CoFe_2O_4$ has only the spinel structure but the others have a mixture of corundum and spinel structures (Figure 1). The result obtained from the analysis of the Mössbouer spectra of the 50 mol% $CoFe_2O_4$ is similar to that of Sawatzky *et al.*[17] (Figure 2). The degree of inversion of the quenched $CoFe_2O_4$ is 0.77, and that of the slowly cooled $CoFe_2O_3$ is 0.96.

A broad band endothermic DTA signal appears in the temperature range from 400 to 1000 °C, and the intensity of the signal increases with temperature (Figure 3).

The plots of log σ vs. 1/T for pure, 10, 20, 30, 40, and 50 mol % $CoFe_2O_4$ systems at a Po_2 of 2×10^{-1} atm and temperatures from 300 to 900 °C are shown in Figure 4. As shown in Figure 4, the electrical conductivity increases with increasing CoO mol% up to 50 mol %. The plots of log σ vs. 1/T for two different 50 mol% $CoFe_2O_4$ samples are shown in Figure 5. One was quenched using 15 °C water after sintering at 1150 °C for 24h, the other was slowly cooled to room temperature at a rate of 50 °C/hr. As shown in Figure 5, at higher temperature, above 600 °C, the slowly-cooled and the quenched samples are equal to each other in electical conductivity and activation energy. At temperatures < 400 °C, the two samples continue to have the same activation energy.

The variations in conductivity with oxygen partial pressure is shown in Figure 6.

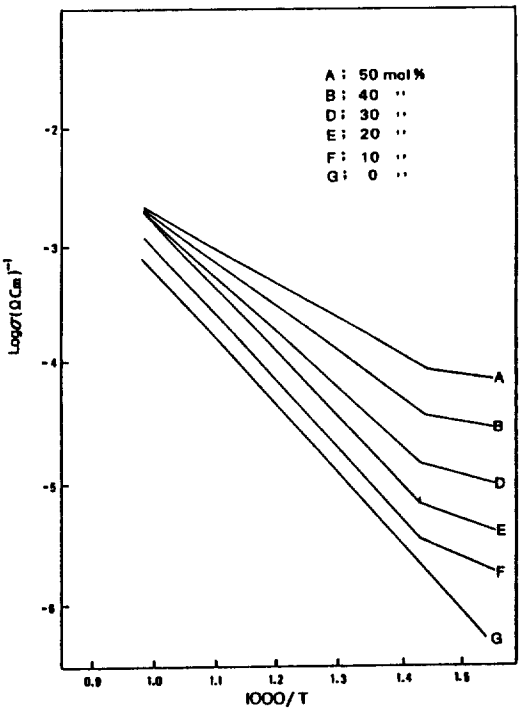

Figure 4. Log conductivity vs. 1000/T for the CoO-α-Fe_2O_3 system.

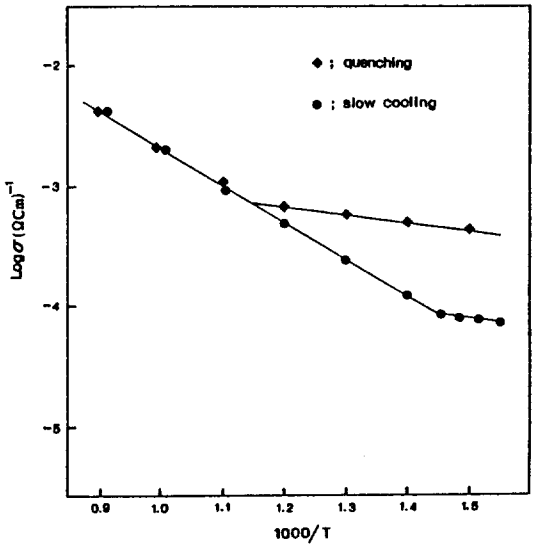

Figure 5. Log conductivity vs. 1000/T for quenched and slow cooled $CoFe_2O_4$.

Discussion

Conduction by electrons or positive holes is found in an electronic semiconductor. Migration of an electron or a hole in a crystal is easy, while diffusion of a cation or anion is dependent on the lattice defects.

It is shown in Figure 4 that the conductivity depends on temperature and CoO mole fraction, converging around 730 °C. This tendency is unusual in metal oxide semiconductors, but is found in bio-organic semiconductors (acriflavine dye complexes such as Vitamin A, adenine, cytosine, and uracil). The fact that the electrical conductivity increases as the CoO mole fraction increases is an antithetic feature for

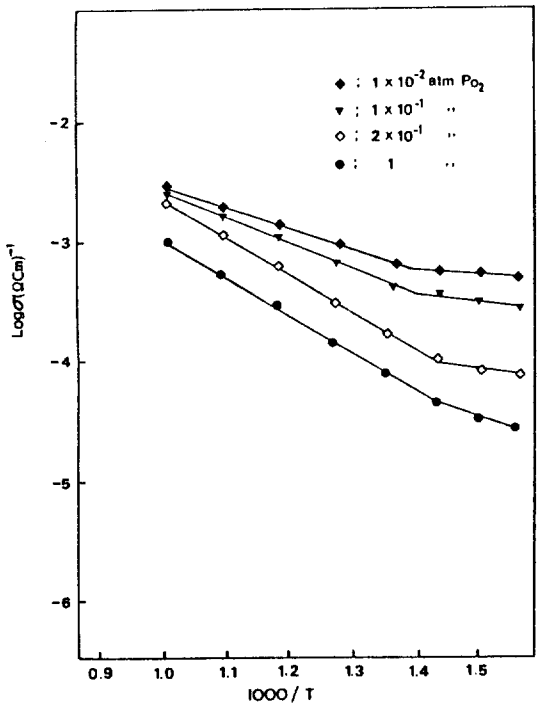

Figure 6. Log conductivity vs. 1000/T for $CoFe_2O_4$ under oxygen partial pressures.

employing very small CoO mole fractions. In the systems of α-Fe_2O_3 doped with CoO containing 0.53-1.51 mol % by Kim *et al.*[49] and of $Co_{0.5}Zn_{0.5}Fe_xO_{4+\epsilon}$ (x = 1.7, 2.0, 2.3, ϵ = − 0.55, 0, +0.55) by Mazen *et al.*[50], as the CoO mole % increased, the electrical conductivity was decreased because the Co ion interrupts the electron hopping due to exchange between Fe^{2+} ions and Fe^{3+} ions. Gillot *et al.*[51] found that in $Co_xFe_{3-x}O_4$ (x = 0.82, 1.0, 1.15, 1.35) conductivity and activation energy varied to a large extent between room temperature to 600 °C, even when the composition deviated from stoichiometry to only a slight degree around $x = 1$. Besides, as a result of further studying on $Zn_xFe_{3-x}O_4$, they reported that the conductivity was decreased more when the ZnO mole fraction was stoichiometrically equivalent, 21.14 wt %, than when $x<1$. Wagner *et al.*[14] reported that the conductivity increased upon adding 0.01-0.935 mol % of TiO_2 to α-Fe_2O_3, which agrees with the data of Jonker[52] and Morin[53]. Jonker[54] reported that $Co_{1-\delta}Fe_{2+\delta}O_4$ ferrite had two regions of electrical conductivity; the higher resistivity region involves Co^{2+} and Co^{3+} ions and the lower resistivity region involves Fe^{2+} and Fe^{3+} ions, respectively. Gillot *et al.*[51] reported that main conduction mechanism in iron excess ferrite was electron hopping from the Fe^{2+} to Fe^{3+} ion, which reduced the activation energy, while for x = 1, the activation energy increased because the Fe^{3+} ion concentration was increased. On the other hand, in Co^{3+} ion excess ferrite, the main conduction mechanism was hole hopping from the Co^{2+} to Co^{3+} ion in a B-site. The Jonker and Gillot results corresponded well with ours which show a bisected two temperature region and similar conductivity values. One can consider the fact that as the CoO mole fraction increased so did the electrical conductivity was due to the electron emitted by Co^{2+} in oxidation to $Co.^{3+}$ Then the emitted electron will reduce the Fe^{3+} ion to Fe^{2+} ion in a B-site. If the Fe^{2+} and Fe^{3+} ion exchange at a B-site is the main conduction machanism, the electrical conductivity will increase with CoO mole %. This suggestion agrees with the conductivity data (Figure 4) in the low temperature range. But the compensation effect in the higher temperature range would result in a scatterring effect for the Co ion as suggested by Kim *et al.*[49]. Therefore, the Co ion is the scattering center as well as the change carrier generator. Thus, it is expected that this cobalt ferrite is a *n*-type semiconductor in which the charge carrier is an electron. The results correspond well to those for the Seebeck effect and oxygen partial pressure dependence.

Table 1. XRD-peak Indexing of $CoFe_2O_4$

2θ	d(Å)	I/I_o	hkl
35.43	2.53	100	311
62.59	1.48	40	440
30.06	2.91	30	220
56.99	1.62	30	711
43.08	2.10	20	400
53.47	1.71	16	422
18.22	4.85	6	111
37.07	2.43	6	222

a = 0.8397 nm

Table 2. Activation Energy for Mole Fraction (X) of CoO

X	high temp. Ea(eV)	low temp. Ea(eV)
0.5	0.63	0.14
0.4	0.72	0.17
0.3	0.83	0.27
0.2	0.89	0.36
0.1	0.92	0.46
0.0	0.92	

The 50 mol% cobalt ferrite was analyzed by DTA. At DTA the continuous endothermic signal indicates that the inverse spinel structure is changed to spinel structure with temperature elevation. Thus the Mössbauer data agrees with the DTA data. In the Mössbauer spectrum of the 50 mol % $CoFe_2O_4$, the difference in degree of inversion implies a site exchange of $Fe_{Td} \rightleftharpoons Co_{Oh}$ or $Co_{Td} \rightleftharpoons Fe_{Oh}$.

As shown in Figure 5, the slopes and conductivity values are the same at temperatures above 600 °C for the two different samples. This implies that the conduction mechanism is the same, and continues to be below 400 °C. But the conductivity of the quenched sample is larger below 600 °C due to the freeze-in effect. The activation energy (0.14 eV) for low temperature region reveals that there is only migration energy for the charge carrier (Fe ion exchange at Oh sites). The electrical conductivity depends on the following equation,

$$\sigma = ne\mu.$$

At constant temperature, charge e is constant, but mobility μ and charge carrier concentration n could be variable with a freeze-in effect. The small value of the degree of inversion (quenched sample) means a large mobility because the exchange probability for Fe ions at B-sites would be increased. And the electrons which come from Co reduction would be frozen. Consequently, the electrical conductivity of the quenched sample is higher than that of the cooled sample in the

lower temperature range (<600 °C). Therefore, we suggest that the degree of inversion greatly affects the mobility.

The dependence of the electrical conductivity on oxygen partial pressure is another characteristic of the cobalt ferrite. The conductivity is increased with decreasing oxygen partial pressure at constant temperature. From conductivity data we could suggest the following equilibrium,

$$Oo \rightleftharpoons 1/2O_2 + V\ddot{o} + 2e'$$

At low Po_2 the equilibrium moves to the right so that the increased electron concentration reduces the Fe^{3+} to Fe^{2+}. Therefore the conductivity should be increased at low oxygen partial pressure. But our data does not show a reasonable oxygen partial pressure dependence (1/n), indicating a defect in the oxide model, possibly because the Co oxidation participated in the charge carrier producing process.

In summary, the electrical conductivity of the cobalt ferrite system depends on the Co mole %, degree of inversion and oxygen partial pressure.

Acknowledgements. The authors are grateful to the Korean Science and Engineering Foundation for financial support and to Professor Ki Hyun Yoon and Yong Bae Kim for useful discussions.

References

1. D. S. Tanhauser, *J. Phys. Chem. Solids,* **23,** 25 (1962).
2. F. J. Morin, *Phys. Rev.,* **93,** 1195 (1954).
3. G. A. Acket and J. Volger, *Physica,* **32,** 1543 (1966).
4. H. J. Van Daal and A. J. Bosman, *Phys. Rev.* **158,** 736 (1967).
5. K. H. Kim and J. S. Choi, *J. Phys. Chem.,* **85,** 2447 (1981).
6. O. N. Salman, *J. Phys. Chem.,* **65,** 550 (1961).
7. O. S. M. Bevan and J. P. Shelton, *J. Chem. Soc. London,* p. 1729, 1948.
8. F. A. Kröger and H. J. Vink, "Solid State Physics", vol. 3, p. 307, *Academi Press,* New York (1956).
9. H. Lord and R. Parker, *Nature,* **188,** 929 (1960).
10. A. J. Bosman and H. J. Van Daal, *Advan. Phys.* **19**(77), 1 (1970).
11. C. Wagner and E. Koch, *Z. Phys. Chem.,* **B32,** 439 (1936).
12. B. Fisher and D. S. Tannhauser, *J. Chem. Phys.,* **44,** 1663 (1966).
13. R. E. Carter and F. D. Richardson, *Trans. AIME,* **200,** 1244 (1954).
14. F. G. Eror and J. B. Wagner Jr, *J. Phys. Chem. Solids,* **29,** 1597 (1968).
15. R. Makkonen, "Vuoritellisuus-Bergshanteringen", p. 26, 1966.
16. M. Gvishi and D. S. Tannauser, *Solid State Comm.,* **8,** 485 (1970).
17. G. A. Sawatzky, F. Van der Woude and A. H. Morrish, *J. Appl. Phys.,* **39**(2), 1204 (1968).
18. J. D. Dunitz, L. E. Orgel, *J. Phys. Chem. Solids,* **3,** 318 (1970).
19. H. L. Yakel, *J. Phys. Chem. Solids,* **41,** 1097 (1980).
20. G. K. Boreskov, V. V. Popovskii, N. E. Lebedeva, V. A. Sazonov, *Kinet. Katal.,* **11,** 1253 (1970), **12,** 979 (1971).
21. Y. Yoneda, S. Makishima and J. Hurssa,X. *Am. Chem. Soc.,* **80,** 4503 (1958).
22. R. G. Squires and G. Parravano, *J. Catalysis,* **2,** 324 (1963).
23. E. Litchner and G. Szalek, *Z. Chem.,* **8,** 314 (1968).
24. W. R. Cares and J. W. Hightower, *J. Catalysis,* **23,** 193 (1971).
25. K. Gwan and R. G. Squires, *Chem. Engng. Progr. Symp. Ser.,* **64,** 24 (1968).
26. R. J. Rennard and W. L. Khel, *J. Catalysis,* **21,** 282 (1971).
27. W. L. Khel and R. J. Rennard, *US Pat.,* **34,** 507,886, (1969).
28. P. N. Rylader and W. J. Zimmerschied, *US Pat.,* **2,** 805,187 (1957).
29. B. Gillot, *Phys. Stat. Sol.* (a), **76,** 601 (1983).
30. G. H. Jonker, *Physica,* **22,** 707 (1956).
31. K. R. Kroshnamurthy, B. Viswanathan and M. V. C. Sastri, *Indian J. Chem.,* **15A,** 205 (1977).
32. G. Bate, "Ferromagnetic Materials" E. P. Wohiforth ED., Chap. 7, North-Holland Publishing Company, (1980).
33. W. Balz, Bodische Anilin and Soda Fabric., Fr. 1,357,866 (1964).
34. L. B. Valdes, *Proc. IRE,* **42,** 420 (1954).
35. J. S. Choi and K. H. Yoon, *J. Phys. Chem.,* **66,** 1308 (1962).
36. J. S. Choi, H. Y. Lee and K. H. Kim, *J. Phys. Chem.,* **77,** 2430 (1977).
37. J. S. Choi, Y. H. Kang and K. H. Kim, *J. Phys. Chem.,* **81,** 2208 (1977).
38. K. H. Kim, H. S. Han and J. S. Choi, *J. Phys. Chem.,* **83,** 1268 (1979).
39. K. H. Kim and J. S. Choi, *J. Phys. Chem.,* **85,** 2447 (1981).
40. K. H. Kim, D. Kim and J. S. Choi, *J. Catal.,* **86,** 219 (1984).
41. K. H. Kim, E. J. Oh and J. S. Choi, *J. Phys. Chem. Solids,* **45,** 1265 (1984).
42. K. H. Kim, H. J. Won and J. S. Choi, *J. Phys. Chem. Solids,* **45,** 1259 (1984).
43. S. H. Lee, G. Heo, K. H. Kim and J. S. Choi, *Int. J. Chem. Kinetics,* **19,** 1 (1987).
44. J. S. Choi, K. H. Kim and S. R. Choi, *Inter. J. Chem. Kinetics.,* **9,** 489 (1977).
45. K. H. Kim, S. H. Lee and J. S. Choi, *J. Phys. Chem. Solids,* **46,** 331 (1985).
46. K. H. Kim, S. H. Park, D.Y. Lim, and J. S. Choi, *J. Phys. Chem. Solids,* **49,** 151 (1988).
47. S. H. Lee, G. Heo, K. H. Kim and J. S. Choi, *J. Appl. Polymer,* **34,** 2537 (1987).
48. S. H. Lee, G. Heo, K. H. Kim and J. S. Choi, *J. Phys. Chem. Solids,* **48,** 895 (1987).
49. K. H. Kim, S. H. Lee and J. S. Choi, *Bull. Korean Chem. Soc.,* **7**(5), 341 (1986).
50. S. A. Masen and M. A. Ahemed, *Phys. Stat. Sol.* (a), **73,** K307 (1982).
51. B. Gillot and F. Jemmali, *Phys. Stat. Sol.* (a), **76,** 601 (1983).
52. G. Jonker and S. Hand Van Honten, "Hslbleiter-problem", F. S. Santer, ed., vol. 6, p. 18. F. Viewegand Sons, Braunschweig, Germany, 1961.
53. F. Morin, *Phys. Rev.,* **83,** 1005 (1951).
54. G. H. Jonker, *Physica,* **22,** 707 (1956).